Multicritical Deconfined Quantum Criticality and Lifshitz Point of a Helical Valence-Bond Phase

Bowen Zhao,[1,*] Jun Takahashi,[2,†] and Anders W. Sandvik[1,2,‡]
[1]Department of Physics, Boston University, 590 Commonwealth Avenue, Boston, Massachusetts 02215, USA
[2]Beijing National Laboratory for Condensed Matter Physics and Institute of Physics, Chinese Academy of Sciences, Beijing 100190, China

(Received 27 May 2020; accepted 6 November 2020; published 17 December 2020)

The $S = 1/2$ square-lattice J-Q model hosts a deconfined quantum phase transition between antiferromagnetic and dimerized (valence-bond solid) ground states. We here study two deformations of this model—a term projecting staggered singlets, as well as a modulation of the J terms forming alternating "staircases" of strong and weak couplings. The first deformation preserves all lattice symmetries. Using quantum Monte Carlo simulations, we show that it nevertheless introduces a second relevant field, likely by producing topological defects. The second deformation induces helical valence-bond order. Thus, we identify the deconfined quantum critical point as a multicritical Lifshitz point—the end point of the helical phase and also the end point of a line of first-order transitions. The helical-antiferromagnetic transitions form a line of generic deconfined quantum-critical points. These findings extend the scope of deconfined quantum criticality and resolve a previously inconsistent critical-exponent bound from the conformal-bootstrap method.

DOI: 10.1103/PhysRevLett.125.257204

The deconfined quantum-critical point (DQCP) is a paradigmatic "beyond Landau" quantum phase transition in two dimensions [1]. Building on field theories for quantum magnets [2–6] and stimulated by intriguing numerical simulations [7,8], the DQCP proposal posits that the transition between an antiferromagnetic (AFM) ground state and a valence-bond solid (VBS, where singlets condense on groups of two or more spins) is continuous and described by spinons coupled to a U(1) gauge field without topological defects. With the symmetry of the spinons extended from SU(2) to SU(N), the proposed CP^{N-1} field theory can be solved for $N \to \infty$. In violation of the Landau rules, which prescribe a first-order transition, the critical exponents including $1/N$ corrections agree remarkably well [9] with simulations [10,11] of lattice models with AFM-VBS transitions for moderately large N.

A contentious aspect of the DQCP scenario is the suggestion that the continuous transition persists down to $N = 2$. This conjecture [1,12] found early support in quantum Monte Carlo (QMC) simulations of the J-Q model, in which the $S = 1/2$ Heisenberg model with exchange J on the square lattice is supplemented by four-spin [13] or six-spin [14] terms Q, illustrated in Figs. 1(a) and 1(b), that induce correlated singlets and lead to VBS order for large Q/J. Many QMC studies of these and other variants of the J-Q model [15–26], as well as related 3D classical loop models [27,28], have characterized the signatures of the DQCP, including an emergent U(1) symmetry of the VBS fluctuations [13,16,19,27]. However, anomalous scaling behaviors have been interpreted by some as precursors to a first-order transition [16,21,29]. Attempts to explain the observations as a weakly first-order "walking" transition invoke a nonunitary conformal field theory (CFT) with a DQCP slightly outside the accessible model space, e.g., in dimensionality different from two [30–35]. In this scenario, the transition reflects the properties of the inaccessible fixed point but eventually, for large lattices, flows away from it. No concrete predictions have been put forward, however, and concurrently further QMC studies have provided compelling evidence of a continuous transition [36].

A puzzling issue is that the critical correlation-length exponent $\nu \approx 0.45$ [24,28,36] violates a bound $\nu > 0.51$ from the CFT bootstrap [37]. We here identify a loophole in this bound and also discover a previously unknown helical valence-bond (HVB) phase. We consider two deformations of the J-Q model and demonstrate that they are

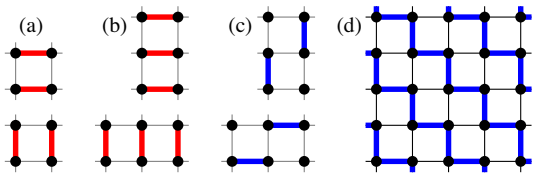

FIG. 1. The multispin columnar Q interactions are products of two (Q_2) in (a) or three (Q_3) in (b) singlet projectors. (c) The Z perturbation consists of all four-spin interactions $(\mathbf{S}_i \cdot \mathbf{S}_j)(\mathbf{S}_k \cdot \mathbf{S}_l)$ with the site pairs ij and kl forming two staggered bonds, as shown, as well as the $\pi/2$ rotated cases. (d) Staircase exchange pattern W, with thick blue and thin black links representing $J(1 \pm h)\mathbf{S}_i \cdot \mathbf{S}_j$.

renormalization-group (RG) relevant at the DQCP. First, we study a four-spin term Z of staggered bond operators; Fig. 1(c). We recently showed that strong staggered interactions lead to a first-order transition [26], likely by suppressing the emergent U(1) symmetry associated with the DQCP [38]. Using QMC simulations, we here show that an infinitesimal Z perturbation is relevant and invalidates the bootstrap ν bound, which is conditional on a single symmetry-preserving relevant field. The second deformation is a staircase J modulation, Fig. 1(d), which is also relevant and evolves the DQCP into a HVB phase.

Model.—We consider the J-Q_2 and J-Q_3 models with exchange J_b on links b connecting nearest-neighbor sites i_b, j_b. Using singlet projectors $P_b = P_{ij} = 1/4 - \mathbf{S}_j \cdot \mathbf{S}_j$, we write the Hamiltonian on periodic lattices with $N = L^2$ spins as

$$H = -\sum_{b=1}^{2N} J_b P_b - Q \sum_{p=1}^{2N} \prod_{\{b_p\}} P_{b_p}, \tag{1}$$

where the products have either two or three singlet projectors in the sets $\{b_p\}$, arranged as in Figs. 1(a) and 1(b).

Defining $g = J/(J+Q)$, the J-Q_2 and J-Q_3 models with uniform $J_b = J$ have AFM-VBS transitions at $g_c \approx 0.0432$ [36] and $g_c \approx 0.400$ [14], respectively. The DQCP has been better characterized in the J-Q_2 model [24,36], and we use it to study the relevance of the infinitesimal staggered bond interactions, Fig. 1(c), and staircase J modulation, Fig. 1(d). The J-Q_3 model is a more robust VBS for large g [19] and we use it to study finite staircase modulation. By universality, our results should apply also to other DQCP systems.

Scaling dimensions.—To characterize the Z and W deformations, we compute corresponding correlation functions in the critical J-Q_2 model. With $H_c = H(g = g_c)$ in Eq. (1), we write the perturbed Hamiltonian as

$$H = H_c + \delta V, \qquad V = \sum_a V(\mathbf{r}_a), \tag{2}$$

where $V(\mathbf{r}_a)$ is a subset of terms of V in a suitable lattice cell. Following standard quantum criticality and RG notation, the correlation function $C_V(\mathbf{r}) = \langle V(\mathbf{r})V(0)\rangle - \langle V(0)\rangle^2$ at $\delta = 0$ should decay as $C_V(\mathbf{r}) \propto r^{-2\Delta_V}$, where Δ_V is the scaling dimension of V. We have used a projector QMC method in the valance-bond basis [39] to calculate $C_V(\mathbf{r})$, using operator cells that will be described below for the two different perturbations. Technical details and additional results are presented in the Supplemental Material [40].

Results for the staggered bonds, $V = Z$, are shown in Fig. 2(a). Here a sum of eight local terms defines the symmetric operator $Z(\mathbf{r})$. The observed power-law decay corresponds to the scaling dimension $\Delta_Z \approx 1.40(2)$, considerably larger than the dimension $\Delta_0 \approx 0.800(4)$ of the previously known primary symmetric scalar operator O_0

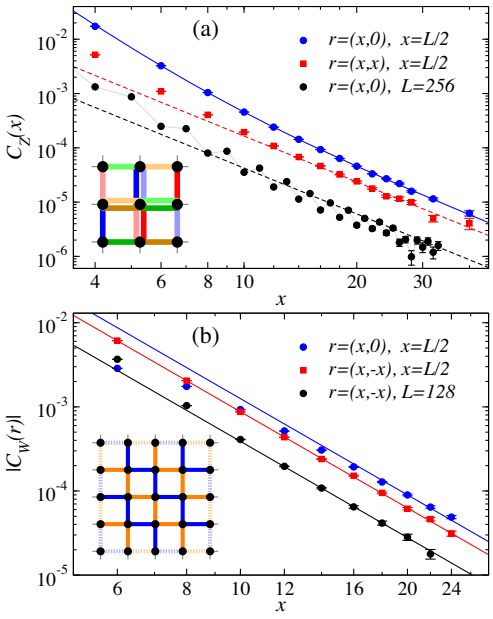

FIG. 2. Correlation functions at $r \propto L/2$ and $r \ll L/2$ of the operators illustrated in the insets. (a) Staggered product operators [Fig. 1(c)], where $Z(\mathbf{r})$ is a sum of eight terms (indicated with different colors). The blue curve is a fit to the $r = (x, 0)$ data for $x = L/2 \geq 6$ of the form $ax^{-2\Delta_0'}(1 + cx^{-\omega})$ giving $\Delta_0' = 1.40(2)$ and $\omega \approx 2.0$. The $L = 256$ data (black symbols) have been divided by 4 for visibility. The dashed lines show the leading power law $x^{-2\Delta_0'}$. (b) Staircase J modulation [Fig. 1(d)] with $W(\mathbf{r})$ defined on a 5×5-site cell with $+\mathbf{S}_i \cdot \mathbf{S}_j$ and $-\mathbf{S}_i \cdot \mathbf{S}_j$ on the blue and orange links, respectively. The dashed edge links indicate prefactors $1/2$ needed for the cell summation in Eq. (2). The correlations being negative, absolute values are shown. A fit (red line) of the form $ax^{-2\Delta_W}$ to the $r = (x, -x)$ data for $x = L/2 \geq 8$ gives $\Delta_W = 1.90(2)$. The other lines have the same slope.

[36]. All correlations are positive and clearly represent the spatially uniform perturbation in Eq. (2). While we can not rigorously prove that Z contains a second primary operator O_0', its scaling dimension matches neither the dimensions $\Delta_0 + n$ $(n = 1, 2, \ldots)$ of the descendants of O_0 nor those of the order parameters O_{VBS} and O_{AFM}, both of which have scaling dimensions of approximately 0.63 [19,28] (see also the Supplemental Material [40]). Thus, we conjecture that a second symmetric primary operator exists. In the Supplemental Material [40] we provide further results supporting this conclusion and show examples of other bond products that exhibit the conventional scaling dimension Δ_0.

It is surprising that an interaction with the symmetries of the unperturbed Hamiltonian can introduce a primary operator not already present in the J-Q model. The most likely scenario is that Z generates topological defects (monopoles). The Q terms in Figs. 1(a) and 1(b) are conducive to the emergent U(1) symmetry that is required within the DQCP scenario and which can be traced to the irrelevance of the quadrupled monopoles associated with the $\mathbb{Z}_4$ symmetric VBS order parameter. Staggered singlets

induced by the Z interaction may counteract the emergent symmetry, as we recently showed with similar terms that, when strong enough, render the AFM-VBS transition clearly first order [26]. Our present results suggest that already an infinitesimal Z causes a first-order transition.

Next, we consider the staircase J modulation, $V = W$, which breaks lattice symmetries. The fourfold degenerate columnar VBS state of the model still retains its $\mathbb{Z}_4$ symmetry, with clocklike angular fluctuations between neighboring states characterized by a complex order parameter $D = |D|e^{i\phi}$ (as we demonstrate in Supplemental Material [40]). The unit cell is doubled when $h > 0$ in Fig. 1(d), but there is no symmetry implying destruction of the DQCP due to Berry phase cancellations, unlike systems such as the bilayer SU(N) model [53]. The W perturbation being irrelevant in the VBS and AFM phases, it could *a priori* also be RG irrelevant at the DQCP, even though it breaks lattice symmetries; in the Supplemental Material [40] we show an example of an irrelevant perturbation breaking the $\pi/2$ lattice rotation symmetry.

Figure 2(b) shows that C_W defined with a 5×5-site cell operator gives $\Delta_W = 1.90(2)$, i.e., the staircase perturbation is also relevant. Thus, the DQCP is unstable, but from the scaling dimension alone we do not know what fixed point the system flows to for a finite W perturbation. We will next show that a new phase opens between the VBS and AFM phases.

HVB phase.—To characterize bond order beyond regular patterns with small unit cells, we here first define a local order parameter coarse grained on a cell of 3×3 spins,

$$T_x(\mathbf{r}) = (-1)^{r_x}(S^z_{\mathbf{r}}S^z_{\mathbf{r}+\hat{x}} + S^z_{\mathbf{r}+\hat{y}}S^z_{\mathbf{r}+\hat{x}+\hat{y}} + S^z_{\mathbf{r}-\hat{y}}S^z_{\mathbf{r}+\hat{x}-\hat{y}} - S^z_{\mathbf{r}}S^z_{\mathbf{r}-\hat{x}} - S^z_{\mathbf{r}+\hat{y}}S^z_{\mathbf{r}-\hat{x}+\hat{y}} - S^z_{\mathbf{r}-\hat{y}}S^z_{\mathbf{r}-\hat{x}-\hat{y}})/6, \quad (3)$$

and $T_y(\mathbf{r}) = T_x(\mathbf{r})(\hat{x} \leftrightarrow \hat{y})$. We will demonstrate that the $J - Q_3$ model with finite staircase modulation $h > 0$ hosts a phase with helical order parameter

$$m(\mathbf{k}(w_x, w_y)) = \sum_{\mathbf{r}} [T_{\hat{x}}(\mathbf{r}) + iT_{\hat{y}}(\mathbf{r})]e^{-i\mathbf{r}\cdot\mathbf{k}(w_x,w_y)}, \quad (4)$$

where (w_x, w_y) are positive integer winding numbers and $\mathbf{k}(w_x, w_y) = 2\pi(w_x, -w_y)/L$. Here the minus sign on w_y applies to the choice of J pattern in Fig. 1(d), where the stairs are directed along the $(1, -1)$ diagonal. The conventional columnar VBS order parameter has $\mathbf{w} = (0, 0)$.

We used the stochastic series expansion (SSE) QMC method [54] at inverse temperature $\beta = L$ to study systems with $0.2 \le h \le 1$. We first visualize the HVB order in Fig. 3, where a bond-centered local angle was extracted from T_x and T_y in short $h = 1$ simulations during which symmetries can be broken. We observe what appears to be long-range order along the diagonal (1, 1) direction and a modulation in the $(1, -1)$ direction, corresponding to winding numbers $\mathbf{w} = (1, 1)$ in Fig. 3(a) and (2, 2) in Fig. 3(b). We find similar behaviors also at smaller h values, and below we will present quantitative results showing how the winding increases versus g at fixed h. We will also demonstrate transitions of the HVB phase into a conventional VBS phase at $g_1(h)$ and an AFM phase at $g_2(h) > g_1(h)$.

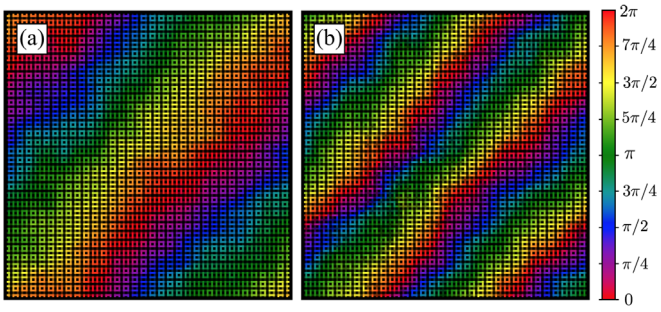

FIG. 3. Spatial dependence of the local VBS order parameter from short SSE runs of $L = 64$ systems at $h = 1$ and $g = 0.25$ (a) and $g = 0.31$ (b). The bar shows the mapping of the angle extracted from bond-centered combinations of $T_x(\mathbf{r})$ and $T_y(\mathbf{r})$ defined in Eq. (3). The brightness indicates the local bond correlation $|\langle S^z_i S^z_j\rangle|$ by a nonlinear map (see Supplemental Material [40]).

The following results were obtained by long SSE runs with bona fide quantum mechanical expectation values averaged over the lattice. We define a correlation function $C_T(\mathbf{r}) = \langle T_x(\mathbf{r})T_x(0)\rangle$ and also study the conventional spin correlation function $C_S(\mathbf{r}) = \langle S^z(\mathbf{r})S^z(0)\rangle$. Examples of both are shown in Fig. 4. As expected from Fig. 3, C_T in the HVB phase is modulated in the $(x, -x)$ direction, while the correlations along (x, x) are always positive and flatten out when $x \to L/2$. In contrast, the spin correlations decay monotonically, faster than a power law in both directions.

Next we consider the squared magnitude of the order parameter (4) for different winding numbers. Figure 5 shows

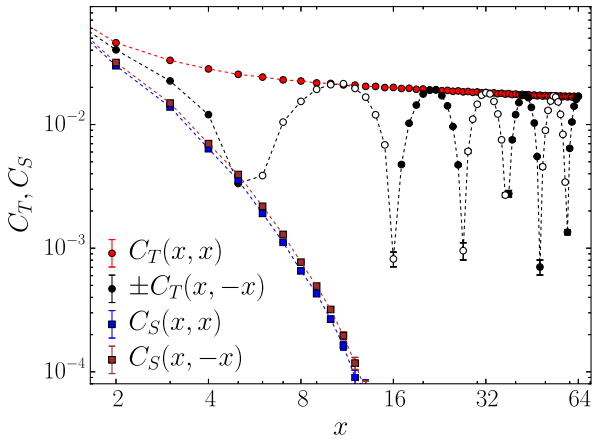

FIG. 4. Bond $C_T(\mathbf{r})$ and spin $C_S(\mathbf{r})$ correlations at $h = 1$ in the diagonal directions of an $L = 128$ system at $g = 0.25$, where $w_x = w_y = 3$. Negative $C_T(x, -x)$ values have been multiplied by -1 and are shown with open circles.

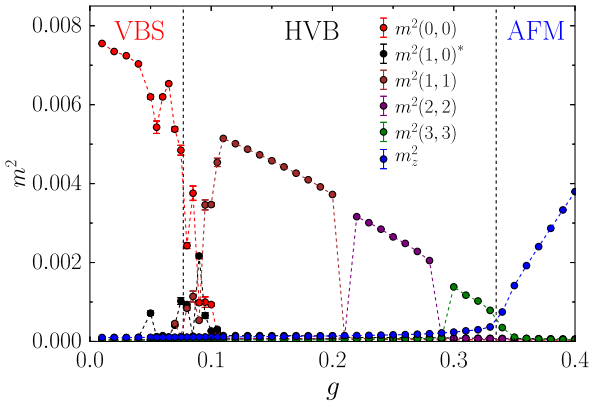

FIG. 5. Helical order parameters in several (w_x, w_y) sectors versus g for an $L = 96$ system at $h = 1$. We have defined $m^2(1,0)^* = m^2(1,0) + m^2(0,1)$, reflecting two degenerate sectors for $g \sim 0.08$–0.09. The staggered AFM order parameter m_z^2 is also shown.

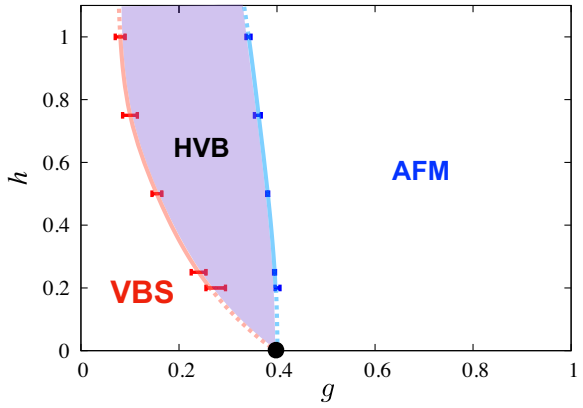

FIG. 6. Phase diagram of the staircase J-Q_3 model. The points with error bars are based on $L = 96$ results (see Supplemental Material [40]) and the lines are guides to the eye. Dotted lines emphasize the unknown shape of the tip of the HVB phase at the multicritical DQCP (circle) and for $h > 1$ (where there is a QMC sign problem).

a scan over g for $L = 96$. The conventional $\mathbf{w} = (0,0)$ VBS order successively gives way to HVB order with higher winding, until $\mathbf{k}^*$ reaches a maximum $\mathbf{k}_{\max}(g)$ and AFM order sets in. The finite-size rounded decays of both the HVB and AFM order parameters suggest a continuous transition. In contrast, the "microtransitions" between different winding numbers exhibit metastability similar to first-order transitions. In the transition regions where all the displayed $m^2(w_x, w_y)$ values are close to zero in Fig. 5, the system fluctuates into winding sectors with $w_x \neq w_y$. Such winding sectors are seen explicitly for $g \sim 0.08$–0.09, where we observe degenerate $\mathbf{w} = (0,1)$ and (1,0) helical order adjacent to the conventional $\mathbf{w} = (0,0)$ VBS phase. In the Supplemental Material [40] we further discuss the metastability and signatures of avoided level crossings in the ground state energy in the neighborhood of winding-number transitions. We also demonstrate that these microtransitions are mediated by the creation of spinon pairs and their subsequent (after winding) destruction. In the thermodynamic limit, we expect the $w_x = w_y$ states to completely dominate the HVB phase.

Phase diagram.—Figure 6 shows the phase diagram constructed from $L = 96$ data such as those in Fig. 5. Results for smaller sizes indicate only minor remaining finite-size effects (see Supplemental Material [40]). The HVB phase narrows with decreasing h and should extend all the way to $h = 0$, on account of the relevance of the infinitesimal staircase perturbation. The DQCP is then a kind of Lifshitz point, where the modulated HVB phase meets the VBS and AFM phases. In contrast to the classical Lifshitz point [55], all three phases are ordered, however. The HVB-AFM transitions replace the classical modulated-disordered transitions and may form a line of DQCPs, as we show in the Supplemental Material [40] by examining critical correlation functions and signatures of emergent U(1) symmetry in the HVB phase. In the thermodynamic limit, the HVB phase at fixed h should contain infinitely many winding sectors. The conventional DQCP approached for $h \to 0$ then has infinite winding degeneracy, as was also argued based on studies of different winding sectors in the standard J-Q model [56].

Discussion.—The CFT bootstrap bound $\nu > 0.51$ [37] for the DQCP has been regarded as conflicting with the QMC value $\nu \approx 0.45$ [24,28,36] and supporting the nonunitary CFT scenario [30–35]. However, the bootstrap argument can also be interpreted differently [37] if the significance of the QMC result is properly recognized: if $\nu < 0.51$, there must be a second relevant field. We have here identified this field as one induced by the staggered bond operators illustrated in Fig. 1(c) and conjecture that it destabilizes the DQCP by topological defects. We expect this effect also with other correlated-singlet projectors that are incompatible with columnar or plaquette VBS states. The values of $1/\nu = 3 - \Delta_0$ and $1/\nu' = 3 - \Delta_0'$ are consistent with the CFT bootstrap [37] and it would be interesting to derive bounds for Δ_{AFM} and Δ_{VBS} given Δ_0 and Δ_0', both with and without the additional assumption of SO(5) symmetry. If there is SO(5) symmetry, Δ_0 and Δ_0' may correspond to crossover and SO(5)-preserving fields, respectively.

We have further demonstrated that the staircase perturbation in Fig. 1(d) is also relevant and opens up a magnetically disordered modulated HVB phase between the conventional VBS and AFM phases. The HVB-AFM transition at $g = g_2$ appears to be a line of generic DQCPs. At the VBS-HVB transition at $g = g_1$ we always observe the smallest nonzero winding number. Thus, in the thermodynamic limit $\mathbf{k}^* \to 0$ continuously and the HVB wavelength diverges when $g \searrow g_1$. When $g \nearrow g_1$, the VBS amplitude does not vanish and its correlation length remains finite. This type of transition is similar to

predictions for certain classical helimagnets [57,58]. Our results extend the known [1] DQCP scenario, suggesting a multicritical point at which the relevance of topological defects can be turned on by a second relevant symmetric field, rendering the VBS-AFM transition first order. Another relevant field induces winding, establishing the conventional DQCP as a Lifshitz type end point of the HVB phase.

The periodic boundary conditions we have used enforce lattice commensurability, and we have not determined whether there can be incommensurate HVB order. The dominant winding vector $\mathbf{k}^*$ may evolve in steps, as known in "devil's staircase" phase diagrams, or continuously, as in "floating" phases [59,60]. In an incommensurate floating HVB phase all correlations would decay as power laws and the distribution of $\mathbf{k}$ would be broadened instead of a δ function at $\mathbf{k}^*$ (i.e., $\mathbf{w}$ would then not be an emergent conserved quantum number). In the future, to settle issues such as these, it would also be useful to study the HVB state under different boundary conditions. We note that, even in classical models it has been very challenging to draw definite conclusions on the properties of modulated and helical phases [58–63].

While transitions between different VBSs have been studied previously [26,64,65], a HVB phase with varying pitch was not considered. The HVB phase with Lifshitz point resembles the tilted phase and "Cantor deconfinement" in a quantum dimer model [66]. However, the spin physics being left out in the dimer model renders two major differences: instead of a DQCP there is Rokhsar-Kivelson point and the critical HVB-AFM line is replaced by first-order transitions of the modulated phase into a staggered dimer phase.

Starting from the critical resonating valence-bond wave function [67,68], it may be possible to construct a wave function with winding and long-range order [69] to describe the HVB phase. In our staircase J-Q model, the winding is induced with a fixed direction and chirality, as we explain further in the Supplemental Material [40].

We thank Ribhu Kaul, Maxim Metlitski, Naoki Kawashima, Yoshihiko Nishikawa, Tin Sulejmanpasic, Chong Wang, and Cenke Xu for valuable discussions, and Duncan Haldane for pointing out the irrelevant perturbation discussed in the Supplemental Material, Sec. 3-C [40]. J. T. acknowledges support by the International Young Scientist Fellowship of the Institute of Physics, Chinese Academy of Sciences, under the Grant No. 202001 and by Boston University's Condensed Matter Theory Visitors Program. A. W. S. was supported by the NSF under Grant No. DMR-1710170 and by Simons Investigator Grant No. 511064. Some of the numerical calculations were carried out on the Shared Computing Cluster managed by Boston University's Research Computing Services.

*bwzhao@bu.edu
†jt@iphy.ac.cn
‡sandvik@bu.edu

[1] T. Senthil, A. Vishwanath, L. Balents, S. Sachdev, and M. P. A. Fisher, Deconfined quantum critical points, Science **303**, 1490 (2004).
[2] F. D. M. Haldane, O(3) Nonlinear σ Model and the Topological Distinction between Integer- and Half-Integer-Spin Antiferromagnets in Two Dimensions, Phys. Rev. Lett. **61**, 1029 (1988).
[3] S. Chakravarty, B. I. Halperin, and D. R. Nelson, Two-dimensional quantum Heisenberg antiferromagnet at low temperatures, Phys. Rev. B **39**, 2344 (1989).
[4] N. Read and S. Sachdev, Valence-Bond and Spin-Peierls Ground States of Low-Dimensional Quantum Antiferromagnets, Phys. Rev. Lett. **62**, 1694 (1989).
[5] N. Read and S. Sachdev, Spin-Peierls, valence-bond solid, and Néel ground states of low-dimensional quantum antiferromagnets, Phys. Rev. B **42**, 4568 (1990).
[6] G. Murthy and S. Sachdev, Action of hedgehog-instantons in the disordered phase of the $2+1$ dimensional CP^{N-1} model, Nucl. Phys. **B344**, 557 (1990).
[7] A. W. Sandvik, S. Daul, R. R. P. Singh, and D. J. Scalapino, Striped Phase in a Quantum XY Model with Ring Exchange, Phys. Rev. Lett. **89**, 247201 (2002).
[8] O. I. Motrunich and A. Vishwanath, Emergent photons and transitions in the O(3) sigma model with hedgehog suppression, Phys. Rev. B **70**, 075104 (2004).
[9] E. Dyer, M. Mezei, S. S. Pufu, and S. Sachdev, Scaling dimensions of monopole operators in the CP^{N_b-1} theory in $2+1$ dimensions, J. High Energy Phys. 06 (2015) 037; Erratum, J. High Energy Phys.03 (2016) 111.
[10] R. K. Kaul and A. W. Sandvik, Lattice Model for the SU(N) Néel to Valence-Bond Solid Quantum Phase Transition at Large N, Phys. Rev. Lett. **108**, 137201 (2012).
[11] M. S. Block, R. G. Melko, and R. K. Kaul, Fate of $\mathbb{CP}^{N-1}$ Fixed Points with q Monopoles, Phys. Rev. Lett. **111**, 137202 (2013).
[12] F. S. Nogueira, S. Kragset, and A. Sudbø, Quantum critical scaling behavior of deconfined spinons, Phys. Rev. B **76**, 220403(R) (2007).
[13] A. W. Sandvik, Evidence for Deconfined Quantum Criticality in a Two-Dimensional Heisenberg Model with Four-Spin Interactions, Phys. Rev. Lett. **98**, 227202 (2007).
[14] J. Lou, A. W. Sandvik, and N. Kawashima, Antiferromagnetic to valence-bond-solid transitions in two-dimensional SU(N) Heisenberg models with multispin interactions, Phys. Rev. B **80**, 180414(R) (2009).
[15] R. G. Melko and R. K. Kaul, Scaling in the Fan of an Unconventional Quantum Critical Point, Phys. Rev. Lett. **100**, 017203 (2008).
[16] F.-J. Jiang, M. Nyfeler, S. Chandrasekharan, and U.-J. Wiese, From an antiferromagnet to a valence bond solid: Evidence for a first-order phase transition, J. Stat. Mech. (2008) P02009.
[17] A. W. Sandvik, Continuous Quantum Phase Transition between an Antiferromagnet and a Valence-Bond Solid in Two Dimensions: Evidence for Logarithmic Corrections to Scaling, Phys. Rev. Lett. **104**, 177201 (2010).

[18] R. K. Kaul, Quantum criticality in SU(3) and SU(4) antiferromagnets, Phys. Rev. B **84**, 054407 (2011).

[19] A. W. Sandvik, Finite-size scaling and boundary effects in two-dimensional valence-bond solids, Phys. Rev. B **85**, 134407 (2012).

[20] K. Harada, T. Suzuki, T. Okubo, H. Matsuo, J. Lou, H. Watanabe, S. Todo, and N. Kawashima, Possibility of deconfined criticality in SU(N) Heisenberg models at small N, Phys. Rev. B **88**, 220408(R) (2013).

[21] K. Chen, Y. Huang, Y. Deng, A. B. Kuklov, N. V. Prokofev, and B. V. Svistunov, Deconfined Criticality Flow in the Heisenberg Model with Ring-Exchange Interactions, Phys. Rev. Lett. **110**, 185701 (2013).

[22] S. Pujari, F. Alet, and K. Damle, Transitions to valence-bond solid order in a honeycomb lattice antiferromagnet, Phys. Rev. B **91**, 104411 (2015).

[23] H. Suwa, A. Sen, and A. W. Sandvik, Level spectroscopy in a two-dimensional quantum magnet: Linearly dispersing spinons at the deconfined quantum critical point, Phys. Rev. B **94**, 144416 (2016).

[24] H. Shao, W. Guo, and A. W. Sandvik, Quantum criticality with two length scales, Science **352**, 213 (2016).

[25] N. Ma, G.-Yu. Sun, Y.-Z. You, C. Xu, A. Vishwanath, A. W. Sandvik, and Z. Y. Meng, Dynamical signature of fractionalization at a deconfined quantum critical point, Phys. Rev. B **98**, 174421 (2018).

[26] B. Zhao, J. Takahashi, and A. W. Sandvik, Tunable deconfined quantum criticality and interplay of different valence-bond solid phases, Chin. Phys. B **29**, 057506 (2020).

[27] A. Nahum, P. Serna, J. T. Chalker, M. Ortuño, and A. M. Somoza, Emergent SO(5) Symmetry at the Néel to Valence-Bond-Solid Transition, Phys. Rev. Lett. **115**, 267203 (2015).

[28] A. Nahum, J. T. Chalker, P. Serna, M. Ortuño, and A. M. Somoza, Deconfined Quantum Criticality, Scaling Violations, and Classical Loop Models, Phys. Rev. X **5**, 041048 (2015).

[29] A. B. Kuklov, M. Matsumoto, N. V. Prokofev, B. V. Svistunov, and M. Troyer, Deconfined Criticality: Generic First-Order Transition in the SU(2) Symmetry Case, Phys. Rev. Lett. **101**, 050405 (2008).

[30] C. Wang, A. Nahum, M. A. Metlitski, C. Xu, and T. Senthil, Deconfined Quantum Critical Points: Symmetries and Dualities, Phys. Rev. X **7**, 031051 (2017).

[31] V. Gorbenko, S. Rychkov, and B. Zan, Walking, weak first-order transitions, and complex CFTs, J. High Energy Phys. 10 (2018) 108.

[32] V. Gorbenko, S. Rychkov, and B. Zan, Walking, Weak first-order transitions, and complex CFTs II. Two-dimensional Potts model at $Q > 4$, SciPost Phys. **5**, 050 (2018).

[33] R. Ma and C. Wang, A theory of deconfined pseudocriticality, Phys. Rev. B **102**, 020407(R) (2020).

[34] A. Nahum, Note on Wess-Zumino-Witten models and quasiuniversality in $2+1$ dimensions, Phys. Rev. B, **102**, 201116(R) (2020).

[35] Y.-C. He, J. Rong, and N. Su, Non-Wilson-Fisher kinks of O(N) numerical bootstrap: From the deconfined phase transition to a putative new family of CFTs, arXiv: 2005.04250.

[36] A. W. Sandvik and B. Zhao, Consistent scaling exponents at the deconfined quantum-critical point, Chin. Phys. Lett. **37**, 057502 (2020).

[37] Y. Nakayama and T. Ohtsuki, Necessary Condition for Emergent Symmetry from the Conformal Bootstrap, Phys. Rev. Lett. **117**, 131601 (2016).

[38] M. Levin and T. Senthil, Deconfined quantum criticality and Néel order via dimer disorder, Phys. Rev. B **70**, 220403(R) (2004).

[39] A. W. Sandvik and H. G. Evertz, Loop updates for variational and projector quantum Monte Carlo simulations in the valence-bond basis, Phys. Rev. B **82**, 024407 (2010).

[40] See Supplemental Material at http://link.aps.org/supplemental/10.1103/PhysRevLett.125.257204 for details of the projector QMC simulations, further analysis of scaling dimensions of various operators, discussion of conservation and breaking of the $\mathbb{Z}_4$ symmetry of the VBS order, explanation of the HVB order visualizations and additional examples, the HVB microtransitions and phase boundaries, critical scaling, evidence for emergent U(1) symmetry in the HVB phase, and the HVB winding mechanism, which include Refs. [41–52].

[41] S. Liang, B. Doucot, and P. W. Anderson, Some New Variational Resonating-Valence-Bond-Type Wave Functions for the Spin-1/2 Antiferromagnetic Heisenberg Model on a Square Lattice, Phys. Rev. Lett. **61**, 365 (1988).

[42] K. S. D. Beach and A. W. Sandvik, Some formal results for the valence bond basis, Nucl. Phys. **B750**, 142 (2006).

[43] L. Liu, H. Shao, Y.-C. Lin, W. Guo, and A. W. Sandvik, Random-Singlet Phase in Disordered Two-Dimensional Quantum Magnets, Phys. Rev. X **8**, 041040 (2018).

[44] J. Takahashi and A. W. Sandvik, Valence-bond solids, vestigial order, and emergent SO(5) symmetry in a two-dimensional quantum magnet, Phys. Rev. Research **2**, 033459 (2020).

[45] M. Oshikawa, Ordered phase and scaling in Z_n models and the three-state antiferromagnetic Potts model in three dimensions, Phys. Rev. B **61**, 3430 (2000).

[46] F. Léonard and B. Delamotte, Critical Exponents Can Be Different on the Two Sides of a Transition: A Generic Mechanism, Phys. Rev. Lett. **115**, 200601 (2015).

[47] T. Okubo, K. Oshikawa, H. Watanabe, and N. Kawashima, Scaling relation for dangerously irrelevant symmetry-breaking fields, Phys. Rev. B **91**, 174417 (2015).

[48] H. Shao, W. Guo, and A. W. Sandvik, Monte Carlo Renormalization Flows in the Space of Relevant and Irrelevant Operators: Application to Three-Dimensional Clock Models, Phys. Rev. Lett. **124**, 080602 (2020).

[49] B. Zhao, P. Weinberg, and A. W. Sandvik, Symmetry-enhanced discontinuous phase transition in a two-dimensional quantum magnet, Nat. Phys. **15**, 678 (2019).

[50] F. D. M. Haldane (private communication). Haldane suggested the irrelevance of this perturbation in the context of a plaquette VBS, but the arguments of preserved $\mathbb{Z}_4$ symmetry are valid also for columnar VBS order.

[51] Y. Tang and A. W. Sandvik, Confinement and Deconfinement of Spinons in Two Dimensions, Phys. Rev. Lett. **110**, 217213 (2013).

[52] C. L. Henley, Relaxation time for a dimer covering with height representation, J. Stat. Phys. **89**, 483 (1997).
[53] R. K. Kaul, Quantum phase transitions in bilayer SU(N) anti-ferromagnets, Phys. Rev. B **85**, 180411(R) (2012).
[54] A. W. Sandvik, Computational studies of quantum spin systems, AIP Conf. Proc. **1297**, 135 (2010).
[55] R. M. Hornreich, The Lifshitz point: Phase diagrams and critical behavior, J. Magn. Magn. Mater. **1518**, 387 (1980).
[56] H. Shao, W. Guo, and A. W. Sandvik, Emergent topological excitations in a two-dimensional quantum spin system, Phys. Rev. B **91**, 094426 (2015).
[57] E. Dzyaloshinskii, Theory of helicoidal structures in anti-ferromagnets. III, Sov. Phys. JETP **20**, 665 (1965).
[58] Y. Nishikawa and K. Hukushima, Phase transitions and ordering structures of a model of a chiral helimagnet in three dimensions, Phys. Rev. B **94**, 064428 (2016).
[59] P. Bak, Commensurate phases, incommensurate phases and the devil's staircase, Rep. Prog. Phys. **45**, 587 (1982).
[60] M. Beccaria, M. Campostrini, and A. Feo, Evidence for a floating phase of the transverse ANNNI model at high frustration, Phys. Rev. B **76**, 094410 (2007).
[61] J. H. van der Merwe, Structure of epitaxial crystal interfaces, Surf. Sci. **31**, 198 (1972).
[62] Y. Togawa, T. Koyama, K. Takayanagi, S. Mori, Y. Kousaka, J. Akimitsu, S. Nishihara, K. Inoue, A. S. Ovchinnikov, and J. Kishine, Chiral Magnetic Soliton Lattice on a Chiral Helimagnet, Phys. Rev. Lett. **108**, 107202 (2012).
[63] P. F. Bienzobaz, N. Xu, and A. W. Sandvik, Modulated phases in a three-dimensional Maier-Saupe model with competing interactions, Phys. Rev. E **96**, 012137 (2017).
[64] A. Vishwanath, L. Balents, and T. Senthil, Quantum criticality and deconfinement in phase transitions between valence bond solids, Phys. Rev. B **69**, 224416 (2004).
[65] L. Balents, L. Bartosch, A. Burkov, S. Sachdev, and K. Sengupta, Putting competing orders in their place near the Mott transition, Phys. Rev. B **71**, 144508 (2005).
[66] E. Fradkin, D. A. Huse, R. Moessner, V. Oganesyan, and S. L. Sondhi, Bipartite Rokhsar-Kivelson points and Cantor deconfinement, Phys. Rev. B **69**, 224415 (2004).
[67] Y. Tang and A. W. Sandvik, and C. L. Henley, Properties of resonating-valence-bond spin liquids and critical dimer models, Phys. Rev. B **84**, 174427 (2011).
[68] P. Patil, I. Dasgupta, and K. Damle, Resonating valence-bond physics on the honeycomb lattice, Phys. Rev. B **90**, 245121 (2014).
[69] Y.-C. Lin, Y. Tang, J. Lou, and A. W. Sandvik, Correlated valence-bond states, Phys. Rev. B **86**, 144405 (2012).